International Journal of Science and Research (IJSR)
ISSN: 2319-7064
ResearchGate Impact Factor (2018): 0.28 | SJIF (2018): 7.426

Prediction of Residual Stresses, Distortions and Microstructure in Effect of Various Welding Processes: A Review

A Pradeep Samuel[1], Nandu Mohan[2]

[1, 2] Amrita Vishwa Vidyapeetham, Amrita University, India
Department of Mechanical Engineering, Amrita School of Engineering, Coimbatore, India

Abstract: ***In this study, the experimental procedure of various welding processes has been explained and the variations in the various properties of weldment due to the influence of several welding parameters were studied. Here, the processes are common to all the conditions such as the welding conditions and material selection criterion. In the present paper, the focus is on presenting and classifying the specified welding process and the changes in the properties of weld in terms of varying parameters applied for welding process. This study allows putting them into proper context based on the new trends in the field of welding. Finally, the variations of the properties of weld with respect to various parameters, defects in weldment and stresses in weldment have been reviewed.***

Keywords: Experimental Procedure, Parameters, Properties, defects, Stresses

1. Introduction

Welding is the process employed for joining materials such as metals or thermoplastics by fusion or non-fusion of metals. It is unlike the lower temperature metal-joining processes such as brazing and soldering, where the melting of the base metal does not take place. In addition to melting the base metal, a filler material is also added to the joint to make the weld pool that cools to form a joint that will be as strong as that of the base material. The Strength of the welded portion of the joint is usually more than that of the strength of the base metal. There are different types of welding processes are being used by the industries today. The welding processes are classified according to the state of the material during welding, as Plastic (or) pressure welding and Fusion (or) non-pressure welding. They can also be classified according to the source of heat, as gas, electric arc, resistance, thermo-chemical, solid state and radiant energy. In that, oxy acetylene or hydrogen welding and air acetylene welding is coming under gas welding processes. The arc welding processes are Carbon arc welding, gas metal arc welding, electro slag welding, submerged arc welding, plasma arc welding, flux cored arc welding, gas tungsten arc welding and atomic hydrogen arc welding. The resistance welding processes are butt welding, resistance butt welding, spot welding, seam welding, projection welding and percussion welding. Thermit welding and atomic hydrogen welding are under thermos-chemical welding processes. The solid state welding processes are friction stir welding, ultrasonic welding, diffusion welding, explosive welding, cold welding, forge welding. Electron beam welding and laser beam welding are coming under radiant energy welding processes. The weld bead geometry depends on the welding parameters such as welding current, voltage, speed, welding force, contact resistance and angle. There will be sudden changes in the metallurgical, geometrical, chemical, mechanical, thermal and magnetic properties of the metal used for welding while there is a variation in the above mentioned welding parameters. There exist some defects and stresses in the welded portion of the metal after rapid solidification of metal after welding.

2. Experimental Procedure

In Gas Tungsten Arc Welding process, the electrodes are connected with the constant power supply which creates an electric arc near the base metal to be melted. The welding parameters have been set according to the requirements in weldment. The workpieces were clamped during the welding process. The weld zone is protected from the atmospheric contaminations by providing the shielding gas around it. Thus, the joint has been made on the surface of the workpieces where it has to be made. This process is commonly employed for joining thin sections of stainless steels and non-ferrous metals such as aluminium, magnesium and copper alloys.

In Gas Metal Arc Welding Process, a constant voltage is applied at the electrode to create an electric arc between the consumable electrode wire and the workpiece. Here, additionally a filler wire used to make the joint over the surface of the specimen. Regarding power supply, either constant direct current or alternating current can be used. Along with the electrode wire, shielding gas will also be provided to prevent the atmospheric contamination of the weldment. The welding parameters have been set according to the required weld. This process is commonly used for welding carbon steel, stainless steel, aluminium, magnesium, copper, nickel, silicon, bronze alloys.

In Shielded Metal Arc Welding, the consumable electrode covered with flux is used to form weld. Here, either alternating current or direct current may be used to produce an electric arc between the electrode and the base metal to be welded. Both the electrode and the base metal melt to form a joint. As the weld was made, the flux coating over the surface of the electrode disintegrates to give vapours and the slag that serves as the shielding gas to provide the weldment from the atmospheric contamination. The major weld able metals for this method are iron, steels and aluminium, copper and nickel alloys can also be used.

In Electron Beam Welding process, the fusion of metal is done by applying a beam of high-velocity electrons on the metals to be joined. The base metal melts and flows as the kinetic energy of the electrons, and transforming into heat energy upon impact. This process is usually done under vacuum conditions to prevent scattering of the electron beam. This process cannot be applied for joining the metals with high-vapour pressure and non-metals.

In Laser Beam Welding process, a laser beam of highly concentrated heat source is used for making narrow and deep welds at high welding rates. This process is based on keyhole or penetration mode of welding. Here, continuous or pulsed laser beam is used continuously to form a sound weld. The depth of penetration depends on the amount of power supplied. Either solid state or gaseous lasers can be used to make joint. Low carbon steels, nickel and titanium alloys can be welded by this process.

In Resistance Spot Welding process, the metal surfaces which are in contact can be joined by the application of heat energy from the resistance to electric current. Specimens are held together under the pressure exerted by the electrodes. Here, the electrodes are to concentrate the current into a small "spot" and to clamp the specimens together at the same time. Then the current is applied through the spot to melt the metal to form weld. Low carbon steels, aluminium and zinc alloys can be welded by this process.

In Friction Stir Welding process, for joining the facing workpieces, a separate tool is used. The heat is being generated between the tool and the workpieces which leads to form a thin layer near the tool. Then the tool combines the workpieces at the joint and the thin layer can be joined under the mechanical pressure. Aluminium alloys can be welded by this process.

In Ultrasonic Welding, the weld can be made by applying high-frequency ultrasonic acoustic vibrations on the workpieces clamped together under pressure. This process is employed for joining plastics and dissimilar materials.

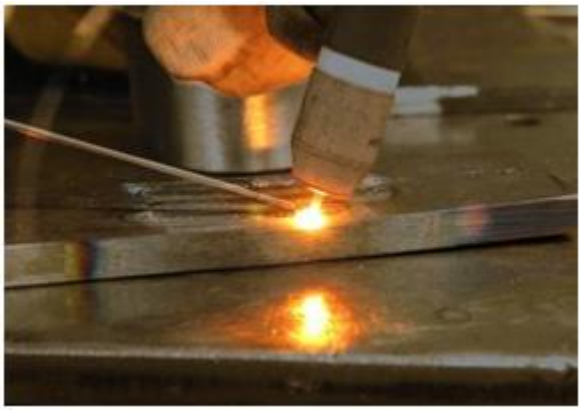

Figure 1: TIG Welding

Figure 2: MIG Welding

Figure 3: Shielded Metal Arc Welding

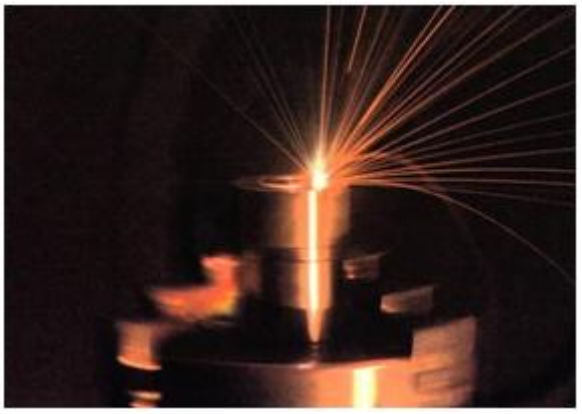

Figure 4: Electron Beam Welding

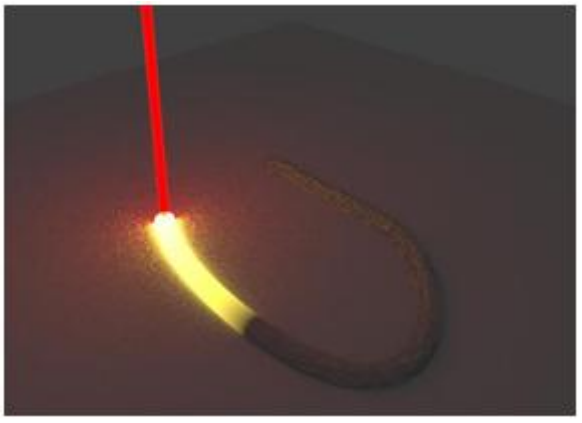

Figure 5: Laser Beam Welding

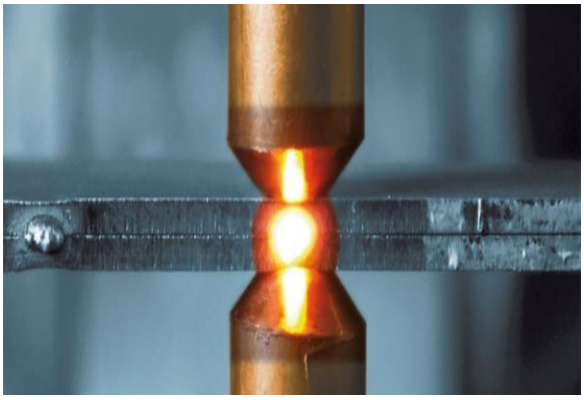

Figure 6: Resistance Spot Welding

Figure 7: Friction Stir Welding

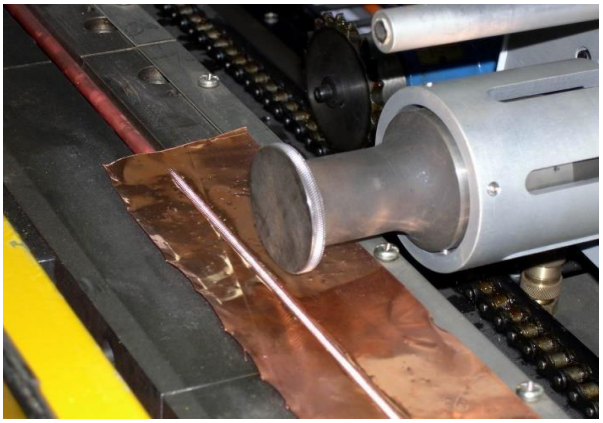

Figure 8: Ultrasonic Welding

3. Results and Discussions

3.1 Determination of Residual stresses

In the weld made using Tungsten Inert Gas Welding process, determination of residual stress and correlated distortions is one of the main goals behind welding heat transfer modeling and the numerical models have a good potential role in this area due to the limitations in NDT techniques used for experimental determination of residual stress. According to V M Joy [1], 2D finite element analysis is used to find the residual stresses for the first time. He analyzed the effect of geometric configuration on residual stresses and compared with results from X-ray diffraction technique. Many others also proposed FEM models to calculate the residual stresses. Most of these researches deal with heat distribution models for thermal profiles of welds and none of them consider the convective currents in the weld pool region while measuring the stress field in the boundaries of the weld pool. The experimental results presented by Chang-Sung Seok [4] proved that the convection in the weld pool region significantly affects the penetration of weld and shape and the stress distributions.

For the joint made by Metal Inert Gas Welding process, According to Afshar, M. R. [5], the longitudinal residual stresses in the plate at mid-span are considered for the nine different welding sequences. The results show that the high tensile stresses are near to the yield stress present at the location of the weldment. At this point, there is a sudden transition in the nature of residual stress from tension to compression. It is seen that the maximum stresses are almost identical for the all welding sequences. This is because of the introduction of more uniform heat input into the material as a result of a proper selection of the welding sequences. Thus, the Welding sequence influences the high residual longitudinal stresses at mid-span of the weldment.

According to Amir Hossein Eslampanah [9], the application of heat over the surface of the workpiece had caused a reduction in the value of residual stresses and the transition occurs, so that the transverse residual stress has good conformity across the weld line direction. Contrary to the transverse residual stress, longitudinal tensile residual stress increases with the increase in heat input in infinite speed along weld line direction. Maximum stress in moving heat source model is higher than that of infinite speed model. This model was employed for the weldment made by Shielded Metal Arc Welding process.

According to Bing Wu [11], the compressive transverse stress occurs on both the top and bottom surfaces, whereas the tensile transverse stress arises in the interior region of the welded plate. A very large compressive transverse stress occurs on the top surface at the location of weld start and end. The longitudinal stress may be tensile within the weld region and tends to zero at the regions which are far from the weldment. The peak tensile longitudinal stress occurs in the interior part of the welded plate. The transverse stress is compressive at the fusion region, increases suddenly with increase in distance from the centerline of the weldment and the value remains close to zero across the total width of the plate. The longitudinal stress which occurs on the top surface of the plate exhibits tensile nature in the weldment with a balanced compressive stress produced in the distant field. This infers the determination of residual stresses for a weld made by Electron Beam Welding process.

According to Kong Fanrong [14], the distributions of the transverse and longitudinal residual stresses are uniform along the centreline of the weldment at the steady-state level. When the heat source approaches the final part, the temperature increases again because of the edge effect. At the edge, the heat lost stimulated by the convection and radiation decreases with an increase in surface area of contact with air. The heat transfer coefficient of the material is higher than that of air leads to the rise of temperature profiles. At the start and end points, there exists large temperature gradient between neighboring elements leads to the greater change in the values of the residual stresses. The

corresponding distribution of residual stresses is achieved when the temperature gradient between the neighboring elements is zero. With an increase in the welding speed, both the transverse and longitudinal residual stresses decreases due to a decrease in the heat input during welding process. The compressive stress is gradually transformed into the tensile stress in the weld zone when the weldment gets cooled down. This is inferred for the weld made by Laser Beam Welding Process.

According to Barsoum Z. [18], the transverse residual stresses were measured in the welded part by X-ray diffraction technique. The measurements were done on the bottom side of the specimen. This represents that the residual stresses at the mid-section are fairly distributed as constant value, except at the start/stop position and that is adequate to determine the residual stresses at this position with a very good accuracy. The axial residual stresses are having tensile nature at weld toe and compressive at weld root gap. This is inferred from the weld made by Resistance Spot Welding process.

According to Sonne, M. R [21], Applying thermal energy in advance to or during the welding process involving both the steady-state and transient thermal conditions has been executed. In short, the idea is to apply moving heat source at all the sides of the moving tool, hence reducing the capacity of plastic yielding in compression during welding process which is major cause for the residual stresses in tension. This is inferred from the weldment made by Friction Stir Welding process.

According to Mehdi Ahmadi [25], the distribution of the residual stresses through the plate thickness is measured with four combinations of transducers with different frequencies. The results for different depths corresponding to the integrating points of the elements. These results are in good agreement with welding sequence which gives the maximum tensile residual stresses generated in the centerline of the weldment and it will be transformed into compressive stress near the HAZ and finally, the stress free zone in the base metal. The result for the residual stresses distribution of the weldment centreline shows a sudden change in the weld start and end points and there is a mild increase in the final third of the weld centreline. This is inferred from the weld made by Ultrasonic Welding process.

3.2 Identification of defects

According to Tian, Liang [2], the angular distortion and transverse shrinkage in the bead-on-plate welding are to be calculated. It is known that the angular distortion first increases to its maximum value at the threshold value of the heat input, then decreases with the increase in heat input, while the transverse shrinkage increases with the increase in the heat input continuously. Here, they have to control the input welding parameters in order to get appropriate outputs of welding distortions for the given welding parameters. It is obtained from the results that a correlation coefficient of about 0.99 has been obtained between the experimental results and predicted results. The percentage errors found for the angular distortion and the transverse shrinkage are also having relatively low values. It infers that this study is capable of making the determination of angular distortion and transverse shrinkage with acceptable accuracy. This is identified from the weld made by Gas Tungsten Arc Welding process.

According to Wang [6], the welding deformation according to the changes made in rib height of T-joint weld was found. The blank gap has a small effect on the determination of the longitudinal bending. However, it can be inferred that it has a significant effect on the angular distortion. Thus, the blank gap is suggested to predict the longitudinal bending and the angular distortion in the T- joint welding. Hence, it is considered as very useful tool, especially for the multi-pass welding process includes the T- joint welding. Other methods may cause unnecessary deflection and lead the results to be unreliable. This is identified from the weldment made by Gas Metal Arc Welding process.

According to Jones L. [12], the distortions can be found out by taking the sequence of processes and by implementing it appropriately based on the suitable welding parameters. This sequence finally executed was used to compare the measured and predicted distortion results. To perform a good comparison, results given by the measurements have to be transformed into a unique reference system. Besides, the measured results may provide additional deformations because of the other machining operations carried out on the different parts assembled. These additional deformations may hide the actual distortions which are only because of the welding process, making the comparison as incoherent. For this reason only, the measured results were post-processed to segregate the deformation related only to the welding process. This post- processing might be done by taking measurements before and after the welding process. This is identified from the weld made by Electron Beam Welding process.

According to Huang [15], the welding deformation is linearly changing with the laser power per length of the weld. The deformations could be reduced by increasing the welding speed. Under the same conditions, the out-of-plane welding deformation is greatly increasing with the length of the plate. This efficiently predicts the magnitude and the mode of induced deformation by considering heat source characteristics, which is effective for accurate computation of results.This is identified from the weld made by Laser Beam Welding process.

According to Yang [19], the distortion of the product could be reduced with minimum cycle time. GA is the best method for solving the discrete problems; it needs single parameter, the fitness value, which is the final distortion of the product. The best welding sequence with minimum Distortion can be found by using GA. A new method has been presented in this that shows how to integrate the minimum distortion sequence and the minimum cycle time path into an entire optimal path. This is identified by Resistance Spot Welding process.

According to Zhang [22], defects can be detected by ultrasonic testing signals based on the compensatory fuzzy neural network and carrying on to the verification. The

result of research provides that because of having the function of compensatory parameter, the possibilities of run into the partial infinitesimal is so small in the network training, so steadily to approach the precision utmost. Carry on categorization of the hour to compensate the network to have the very fast learning speed, but also may realize the accurate recognition of the defects. Through the experiment results, this network will be verified for rate of high accuracy to deliver the defect of the joint and to satisfy the demand of the engineering applications. This is identified from the weldment made by Friction Stir Welding process.

3.3 Variations in weld pool geometry

According to Ohshima K. [3], the weld pool is simulated by the finite difference method based on the theory of heat conduction. The weld pool width and the cooling rate were calculated under various types of the welding current and the welding speed. It is mandatory to control the weld pool width and cooling time for attaining the suitable weld pool width, the perfect crystalline structure and the proper hardness after the welding process. Hence, the welding speed and welding current are found to obtain the constant weld pool width and cooling rate by using the weld pool model. This is inferred from the weld pool made by Gas Tungsten Arc Welding process.

According to Zhang [8], a system with sensor and controller is set up for GMAW process. This system includes welding system, vision sensing system, neural network predicting system and fuzzy control system. A fuzzy logic controller is constructed for the prediction of level of weld penetration. Some fuzzy logics are being proposed by simulating the manual controlled process. It may be seen that the relations between the inputs and outputs of the fuzzy controller is non-linear. A simulation system is set up with neural networks of top side and backside weld pool parameters to make the fuzzy controller designing and verifying as easier. The simulated rand controlled results show this simulation system is demonstrated. This is inferred from the weld pool made by Gas Metal Arc Welding process.

According to Datta G. L [10], the weld beads deposited on specimens using either a high arc-travel rate or low arc-power produces very poor fusion. Use of either preheated specimens or low arc-travel rate or high arc-power yielded provides better fusion. Both the bead height and the bead width are decreasing with the increase in arc-travel rate but the decrease in height is comparatively high to make a flat bead with a higher arc-travel rate. At the constant arc-length and a higher electrode feed rate, the bead height did not change significantly but the bead width increases rapidly. An increase in arc-length keeps the electrode feed rate as constant which results in an increase in the bead width and decrease in the bead height. An increase in the arc-length from short to medium by increasing arc-power and keeping the electrode feed rate as constant which results initially in a quick increase in the areas and depth of penetration of weldment. The ratio of the depth of penetration of weld and the arc-length represents that neither too small nor too long arc-length is desirable from the point of view of appropriate penetration and effective heat utilization. The penetration and HAZ increases with the increase in the electrode feed rate and keeping arc-length as constant. This is inferred from the weld pool obtained by Shielded Metal Arc Welding process.

According to Vidyut Dey [13], both the back-propagation neural networks (BPNN) as well as genetic–neural system (GA-NN) were developed to determine weld bead-profiles of electron beam welding process. Both of them were found to give good predictions of the weld-bead profiles. However, the BPNN showed a slightly better performance compared to the GA-NN in prediction of the bead-profiles. It is because of the performance of BPNN and GA-NN is dependent on the nature of error surface. This is inferred from the weld pool made by Electron Beam Welding process.

According to G.Buvanashekaran [16], the shape of weld is almost circular for a straight beam of light and it becomes elliptical in nature if the beam is tilted from the vertical axis. At the constant beam of power and beam exposure time, the depth of penetration and the bead width decreases with the decrease in beam incident angle from 85º to 75º, however, the bead length increases with the decrease in the incident angle. The weld pool shape corresponding to high laser power of is nearly semi-circular, which leads to conduction mode welding. But for laser powers, the depth of penetration increases suddenly in comparison with bead length and bead width. Comparison of experimental and simulation results reveal a very good association for depth of penetration, bead length and bead width, the overall percentage of error observed is very small. This is inferred from the weld pool made by Laser Beam Welding process.

3.4 Prediction of microstructure

According to Grujicic M. [7], the micro structural- evolution interpretation presented is revealed that the nature of origin of the phase transformations encountered and their thermodynamic/ kinetic relations were drastically different for the different material points occurring in the fusion zone and in the heat affected zone. At the same time, different micro structural evolutions functional relationships have to be applied to the material points occurring in these two portions of weld zone. Once these relations have obtained the results tending to the spatial difference of the phase volume fraction within the fusion zone and the heat affected zone, these results are associated to produce phase volume-fraction contour plots graphs, one contour plot for the each Crystalline phase has been analyzed. This is being observed in the weld made by Gas Metal Arc Welding process.

According to Ganguly S. [17], the micro structural analysis shows that the composite layer is composed of a needle shaped FeAl3 on the Al side and the tongue shaped Fe2Al5 on side of steel. The Fe2Al5 is as much thicker as compared to FeAl3. The initial increase in the mechanical strength with the specific point of energy has been noted which can be attributed to the increase in the wetting area with the increase in the specific point of energy. Although the gradual increase in the thickness of the layer has also been determined in that range it seems to get the advantage leading to the increase in the wetting area brings out the adverse impact of the increase in thickness of the layer. This has been observed from the weld made by Laser Beam

Welding process.

According to Xiaojian [20], the curve of moving resistance indicates that the entire process of the nugget growth is comprised of the initial stage, growth stage and the stable stage. The Different types of the nugget growth shows the diverse curves of the moving resistance, which is also useful means to determine the quality of nugget. Only the energy is provided for the nugget growth and an adequate nugget is produced, the entire process of the nugget growth is comprised of the three stages totally. The variations made in the welding parameters affects the process of the nugget growth. The Larger welding current and the larger electrode force are promoting the rate of the nugget growth. This is observed from the weld made by Resistance Spot Welding process.

According to Sumitesh [24], it has been executed that by using CAFE modeling approach, the micro structural features and formation behavior of the welded zone may be predicted with good accuracy during solid state welding process. The grain size is the only feature that can be controlled by CAFE modeling in the present work displayed in the simple model. The grain size determinations agree well with theoretical results of the similar grade combination and the dissimilar grade combination respectively. The modification in the average grain size with increase in the welding speed is clearly observed in the experimental data analysis that has been successfully captured by the present model. The dislocation density determinations through the grain size evolution also matches well with the experimental data. The analytical model shows the better dislocation density prediction than empirical model when it is compared with the experimental model. This is observed from the weldment made by Friction Stir Welding process.

4. Conclusion

The welding research began in 1920 itself for developing new trends to increase the efficiency of the weld. Still the research is going to improve the soundness of weld by various welding methods. In this study, the overview of the prediction of residual stresses, distortions and the Microstructure by various processes under various welding conditions has been explained. The ways to improve the effectiveness of both the process and the product is detailed here. Hence, this kind of reviewing of processes makes the certain developments in the process and provides useful information while looking for research aspects.

5. Scope for Future Work

From the beginning itself, only limited research has been carried out to interconnect the fundamentals of welding processes and characteristics of the welded joint, in order to avoid the discrepancies. Only experimental details are available for explaining the effect of welding on various materials and no other methods are developed for accounting these details. So, it will give a good start for the research and development of the welding processes and also it paves a way for the existence of newer welding process.

References

[1] V. M. J. Varghese, M. R. Suresh, and D. S. Kumar, “Recent developments in modeling of heat transfer during TIG welding — a review,” pp. 749–754, 2013.
[2] L. Tian, Y. Luo, Y. Wang, and X. Wu, “Prediction of transverse and angular distortions of gas tungsten arc bead- on-plate welding using artificial neural network,” *Mater. Des.*, vol. 54, pp. 458–472, 2014.
[3] J. Bingzhe, L. Wenhuan, and K. Ohshima, “Control of weld pool width and cooling rate in circumferential GTA welding of a pipe by using neural network model,” *IEEE Conf. Ind. Autom. Control Emerg. Technol. Appl.*, pp. 41– 46, 1995.
[4] R. Keivani, M. Jahazi, T. Pham, A. R. Khodabandeh, and M. R. Afshar, “Predicting residual stresses and distortion during multisequence welding of large size structures using FEM,” *Int. J. Adv. Manuf. Technol.*, vol. 73, no. 1–4, pp. 409–419, 2014.
[5] M. Hashemzadeh, B. Q. Chen, and C. GuedesSoares, “Numerical and experimental study on butt weld with dissimilar thickness of thin stainless steel plate,” *Int. J. Adv. Manuf. Technol.*, vol. 78, no. 1–4, pp. 319–330, 2015.
[6] C. Wang, Y. Kim, and J. Kim, “Comparison of FE Models to Predict the Welding Distortion in T-Joint Gas Metal Arc Welding Process,” vol. 15, no. 8, pp. 1631–1637, 2014.
[7] M. Grujicic, S. Ramaswami, J. S. Snipes, R. Yavari, A. Arakere, C. F. Yen, and B. A. Cheeseman, “Computational modeling of microstructural-evolution in AISI 1005 steel during gas metal arc butt welding,” *J. Mater. Eng. Perform.*, vol. 22, no. 5, pp. 1209–1222, 2013.
[8] Z. Yan, G. Zhang, and L. Wun, “Simulation and Controlling for Weld Shape Process in P-GMAW Based on Fuzzy Logic,” pp. 2078–2082, 2011.
[9] A. H. Eslampanah, M. E. Aalami-aleagha, and S. Feli, “3-D numerical evaluation of residual stress and deformation due welding process using simplified heat source models †,” vol. 29, no. 1, pp. 341–348, 2015.
[10] D. S. Nagesh and G. L. Datta, “Prediction of weld bead geometry and penetration in shielded metal-arc welding using artificial neural networks,” *J. Mater. Process. Technol.*, vol. 123, no. 2, pp. 303–312, 2002.
[11] M. Society, “Numerical Investigation of Residual Stress in Thick Titanium Alloy Plate Joined with Electron Beam Welding,” vol. 41, no. October, 2010.
[12] J. Guirao, E. Rodr??guez, A. Bay??n, F. Bouyer, J. Pistono, and L. Jones, “Determination through the distortions analysis of the best welding sequence in longitudinal welds VATS electron beam welding FE simulation,” *Fusion Eng. Des.*, vol. 85, no. 5, pp. 766–779, 2010.
[13] V. Dey, D. K. Pratihar, and G. L. Datta, “Prediction of weld bead profile using neural networks,” *Proc. - 1st Int. Conf. Emerg. Trends Eng. Technol. ICETET 2008*, pp. 581– 586, 2008.
[14] W. Liu, J. Ma, F. Kong, S. Liu, and R. Kovacevic, “Numerical Modeling and Experimental Verification of Residual Stress in Autogenous Laser Welding of High- Strength Steel,” *Lasers Manuf. Mater. Process.*,vol. 2, no. 1, pp. 24–42, 2015.

[15] H. Huang, J. Wang, L. Li, and N. Ma, "Journal of Materials Processing Technology Prediction of laser welding induced deformation in thin sheets by efficient numerical modeling," *J. Mater. Process. Tech.*, vol. 227, pp. 117–128, 2016.
[16] N. S. Shanmugam, G. Buvanashekaran, and K. Sankaranarayanasamy, "Some studies on weld bead geometries for laser spot welding process using finite element analysis," *Mater. Des.*, vol. 34, pp. 412–426, 2012.
[17] S. Meco, G. Pardal, S. Ganguly, S. Williams, and N. McPherson, "Application of laser in seam welding of dissimilar steel to aluminium joints for thick structural components," *Opt. Lasers Eng.*, vol. 67, pp. 22–30, 2015.
[18] Z. Barsoum and A. Lundbäck, "Simplified FE welding simulation of fillet welds - 3D effects on the formation residual stresses," *Eng. Fail. Anal.*, vol. 16, no. 7, pp. 2281– 2289, 2009.
[19] H. Yang and H. Shao, "Journal of Materials Processing Technology Distortion-oriented welding path optimization based on elastic net method and genetic algorithm," vol. 209, pp. 4407–4412, 2009.
[20] L. Yi, R. Wan, X. Xiaojian, and Z. Yang, "Journal of Materials Processing Technology Study on the nugget growth in single-phase AC resistance spot welding based on the calculation of dynamic resistance," *J. Mater. Process. Tech.*, vol. 229, pp. 492–500, 2016.
[21] Z. Lin, Y. Zhang, G. Chen, and Y. Li, "Study on Real-Time Measurement of Nugget Diameter for Resistance Spot Welding Using a Neuro-Fuzzy Algorithm," pp. 2230–2233, 2004.
[22] J. H. Hattel, M. R. Sonne, and C. C. Tutum, "Modelling residual stresses in friction stir welding of Al alloys???a review of possibilities and future trends," *Int. J. Adv. Manuf. Technol.*, vol. 76, no. 9–12, pp. 1793–1805, 2014.
[23] X. I. N. Yin and Z. Zhang, "DEFECT RECOGNIZED SYSTEM OF FRICTION WELDING BASED ON," no. July, pp. 12–15, 2009.
[24] S. R. Valvi, A. Krishnan, and S. Das, "Prediction of microstructural features and forming of friction stir welded sheets using cellular automata finite element (CAFE) approach," 2015.
[25] Y. Javadi, M. Akhlaghi, and M. A. Najafabadi, "Using finite element and ultrasonic method to evaluate welding longitudinal residual stress through the thickness in austenitic stainless steel plates," *Mater. Des.* vol. 45, pp. 628–642, 2013.